NRC Publications Archive
Archives des publications du CNRC

Charge-spin correlation in van der Waals Antiferromagnet NiPS3
Kim, So Yeun; Kim, Tae Yun; Sandilands, Luke J.; Sinn, Soobin; Lee, Min-Cheol; Son, Jaeseok; Lee, Sungmin; Choi, Ki-Young; Kim, Wondong; Park, Byeong-Gyu; Jeon, C.; Kim, Hyeong-Do; Park, Cheol-Hwan; Park, Je-Geun; Moon, S. J.; Noh, T. W.

This publication could be one of several versions: author’s original, accepted manuscript or the publisher’s version. / La version de cette publication peut être l’une des suivantes : la version prépublication de l’auteur, la version acceptée du manuscrit ou la version de l’éditeur.
For the publisher’s version, please access the DOI link below./ Pour consulter la version de l’éditeur, utilisez le lien DOI ci-dessous.

Publisher’s version / Version de l'éditeur:
https://doi.org/10.1103/PhysRevLett.120.136402
Physical Review Letters, 120, 13, 2018-03-27

NRC Publications Archive Record / Notice des Archives des publications du CNRC :
https://nrc-publications.canada.ca/eng/view/object/?id=f9599632-84c2-4040-8c9b-2a73ae61ecc4
https://publications-cnrc.canada.ca/fra/voir/objet/?id=f9599632-84c2-4040-8c9b-2a73ae61ecc4

Access and use of this website and the material on it are subject to the Terms and Conditions set forth at
https://nrc-publications.canada.ca/eng/copyright
READ THESE TERMS AND CONDITIONS CAREFULLY BEFORE USING THIS WEBSITE.

L’accès à ce site Web et l’utilisation de son contenu sont assujettis aux conditions présentées dans le site
https://publications-cnrc.canada.ca/fra/droits
LISEZ CES CONDITIONS ATTENTIVEMENT AVANT D’UTILISER CE SITE WEB.

Questions? Contact the NRC Publications Archive team at PublicationsArchive-ArchivesPublications@nrc-cnrc.gc.ca. If you wish to email the authors directly, please see the first page of the publication for their contact information.

Vous avez des questions? Nous pouvons vous aider. Pour communiquer directement avec un auteur, consultez la première page de la revue dans laquelle son article a été publié afin de trouver ses coordonnées. Si vous n’arrivez pas à les repérer, communiquez avec nous à PublicationsArchive-ArchivesPublications@nrc-cnrc.gc.ca.

PHYSICAL REVIEW LETTERS **120,** 136402 (2018)

Charge-Spin Correlation in van der Waals Antiferromagnet NiPS$_3$

So Yeun Kim,[1,2] Tae Yun Kim,[2,3] Luke J. Sandilands,[1,2,§] Soobin Sinn,[1,2] Min-Cheol Lee,[1,2] Jaeseok Son,[1,2]
Sungmin Lee,[1,2] Ki-Young Choi,[1,2] Wondong Kim,[4] Byeong-Gyu Park,[5] C. Jeon,[6] Hyeong-Do Kim,[1,2]
Cheol-Hwan Park,[2,3] Je-Geun Park,[1,2,*] S. J. Moon,[7,†] and T. W. Noh[1,2,‡]
[1]*Center for Correlated Electron Systems, Institute for Basic Science (IBS), Seoul 08826, Republic of Korea*
[2]*Department of Physics and Astronomy, Seoul National University (SNU), Seoul 08826, Republic of Korea*
[3]*Center for Theoretical Physics, SNU, Seoul 08826, Republic of Korea*
[4]*Korea Research Institute of Standards and Science (KRISS), Daejeon 34113, Republic of Korea*
[5]*Pohang Accelerator Laboratory, Pohang University of Science and Technology (POSTECH), Pohang 37673, Republic of Korea*
[6]*Advanced Nano-Surface Group, Korea Basic Science Institute (KBSI), Daejeon 34133, Republic of Korea*
[7]*Department of Physics, Hanyang University, Seoul 04763, Republic of Korea*

(Received 25 June 2017; revised manuscript received 29 September 2017; published 27 March 2018)

Strong charge-spin coupling is found in a layered transition-metal trichalcogenide NiPS$_3$, a van der Waals antiferromagnet, from studies of the electronic structure using several experimental and theoretical tools: spectroscopic ellipsometry, x-ray absorption, photoemission spectroscopy, and density functional calculations. NiPS$_3$ displays an anomalous shift in the optical spectral weight at the magnetic ordering temperature, reflecting strong coupling between the electronic and magnetic structures. X-ray absorption, photoemission, and optical spectra support a self-doped ground state in NiPS$_3$. Our work demonstrates that layered transition-metal trichalcogenide magnets are useful candidates for the study of correlated-electron physics in two-dimensional magnetic materials.

DOI: 10.1103/PhysRevLett.120.136402

Layered van der Waals (vdW) materials, such as graphene and transition-metal (TM) dichalcogenides, have attracted much attention over the last decade [1–3]. A remarkable advantage of these materials is that they can be mechanically exfoliated to produce two-dimensional (2D) crystals [1–3]. The intriguing collective quantum phenomena found in 2D vdW materials include charge density waves and superconductivity [4–8]. These observations open a new approach for novel device applications through the manipulation of collective quantum states in atomically thin 2D phases [3,6,9]. Despite extensive research on vdW materials, it is striking that very few studies have focused on magnetic 2D vdW materials.

Only recently has attention focused on new magnetic 2D vdW materials of ternary transition-metal trichalcogenide (TMTC) families, such as CrBTe$_3$ (B = Si or Ge) and TMPX_3 ($TM = 3d$ TMs; X = chalcogens) [10–12]. These TMTC samples exhibit various magnetic orderings: ferromagnetic (FM), zig-zag antiferromagnetic (AF), Néel AF, and stripy AF [10–16]. Moreover, all three key magnetic Hamiltonians—i.e., Ising, XY, and Heisenberg types—are realized in TMPX_3 [13–17]. Additionally, long-range magnetic ordering has recently been reported to persist in the atomically thin limit, e.g., monolayer FePS$_3$ and bilayer CrGeTe$_3$ [10,14,18]. Thus, it has become clear that the TMTC families, i.e., layered vdW magnets, are excellent candidates for exploring intriguing phenomena related to 2D magnetism, which will ultimately pave the way for novel applications in spintronics.

Compared with other nonmagnetic vdW materials, these new magnetic vdW materials offer a unique opportunity to explore strongly correlated electron systems in the 2D limit. Electronic correlation physics has been widely investigated in TM oxides, where the coupling of charge-spin-orbital-lattice degrees of freedom leads to various emergent phenomena [19–21]. One of the most intriguing phenomena due to electronic correlations is observed in quasi-2D materials, i.e., high-transition-temperature (T_c) superconductivity [22,23]. Over the past few decades, researchers have attempted to unravel correlation physics in 2D materials of heterostructure interfaces and/or oxide ultrathin films, and have reported a variety of interesting observations [24–28]. Layered magnetic vdW materials offer an interesting platform for exploring correlation-induced phenomena. Intrinsic magnetism in TMTC implies the presence of localized electrons, so correlation physics is expected in these vdW materials. The electronic structure of TMTC can provide insights into the electronic correlations in layered magnetic vdW materials. However, few experimental studies have focused on the electron correlation in TMTC.

In this Letter, we report on the electronic structure of bulk NiPS$_3$ single crystal, a TMTC antiferromagnet in which the electronic and spin (or magnetic) structures are closely related. Using optical spectroscopy techniques, we observed clear anomaly in the optical spectral weight at the Néel temperature, driven mainly by the magnetic ordering, which is a hallmark of correlated electronic systems [21,29]. Subsequent x-ray absorption and photoemission studies, along with cluster model calculations, also revealed that $\mathrm{NiPS_3}$ is a self-doped negative charge transfer (NCT) insulator. That is, the ligand (sulfur ions) has a strong holelike character due to NCT energy, analogous to the hole-doped high-T_c cuprates and Kondo insulators [30,31]. Such an intriguing electronic and magnetic ground state was also confirmed by density functional theory (DFT) with effective Coulomb interaction (U_{eff}) calculations. Our findings indicate that $\mathrm{NiPS_3}$ is a unique vdW magnet exhibiting clear evidence of strong correlation and NCT behavior.

High-quality single crystals of $\mathrm{NiPS_3}$ were grown by a chemical vapor transport method, as described previously [32,33]. For optical measurements, we used a 55-μm-thick single crystal and an M-2000 ellipsometer (J. A. Woollam Co.). Ni L-edge x-ray absorption (XAS) spectra were obtained using scanning transmission x-ray microscopy (STXM) at beam line 10A of Pohang Light Source (PLS) II. We carried out the DFT + U_{eff} calculations using the QUANTUM ESPRESSO package [34,41–47].

$\mathrm{NiPS_3}$ is one of the transition-metal phosphorous trichalcogenides ($\mathrm{TMP}X_3$) with an AF long-range ordering. It has a monoclinic structure with C_{2h}^3 symmetry and features edge-sharing $\mathrm{NiS_6}$ octahedra arranged on a honeycomb lattice [32,48]. At the center of the honeycomb lattice, two P atoms are located above and below the TM plane. They are covalently bonded to the S atoms, forming a $(\mathrm{P_2S_6})^{4-}$ anion [48,49]. The magnetic moments of Ni ions are known to be aligned in a so-called "zig-zag" pattern; i.e., chains of ferromagnetically coupled spins are arranged antiferromagnetically [16], as shown in the inset of Fig. 1(a). Our in-plane magnetic susceptibility $\chi(T)$ shows an AF magnetic anomaly at the Néel temperature ($T_N \sim 154$ K) [Fig. 1(b)].

The optical conductivity spectra $\sigma_1(\omega)$ show that $\mathrm{NiPS_3}$ is an insulator with an optical gap of about 1.8 eV [Fig. 1(a)]. At the same time, there are strong narrow absorption peaks near 2.2, 3.5, and 4.6 eV [labeled A, B, and C, respectively, in Fig. 1(a)]. Below the gap, there are two additional weak peaks near 1.1 and 1.7 eV, denoted as α and β, respectively [see Supplemental Material (c-1) [34]]. For comparison, NiO, which has the same formal valence of Ni (+2) as $\mathrm{NiPS_3}$, is reported to have weak on-site $d-d$ transitions at 1.13 and 1.75 eV [51]. Due to the similarities in the energy positions and strengths of the peaks, it is most likely that the α and β peaks are the on-site $d-d$ transitions, a transition within one Ni ion. It should be noted that the hybridization of Ni $3d$ orbitals with S $3p$ can provide a much larger bandwidth than that with O $2p$ in NiO. Nonetheless, the narrowness of the A, B, and C peaks, in addition to the existence of the α and β peaks, suggests the presence of well-localized Ni $3d$ orbital states near the Fermi energy (E_F) in the electronic structure.

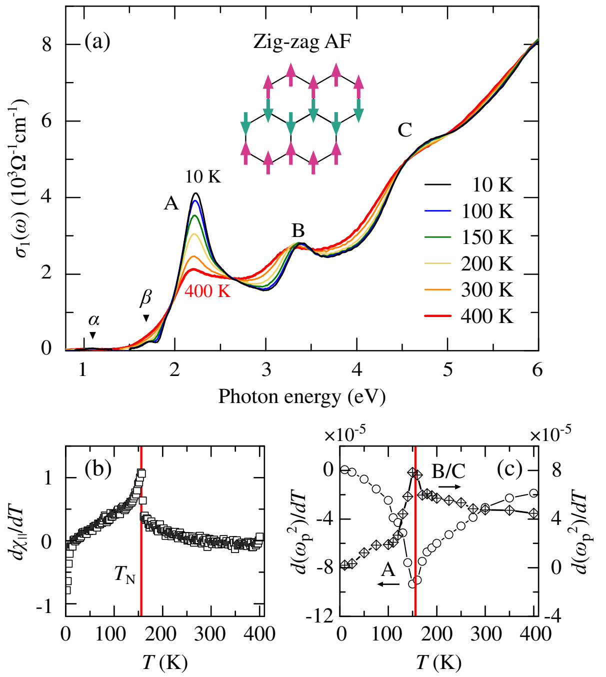

FIG. 1. (a) Real part of the optical conductivity $\sigma_1(\omega)$ of $\mathrm{NiPS_3}$ measured between 10 and 400 K [50]. The three main optical transitions are labeled A, B, and C. Two weak on-site $d-d$ transitions (α and β) are located below 2 eV. The inset shows the schematic diagram of the zig-zag antiferromagnetic ordering, where the honeycomb lattice of Ni ions is shown by black lines, and the spin is depicted as an arrow in each site. (b) The first derivative of magnetic susceptibility (χ) with respect to temperature measured under in-plane bias fields on $\mathrm{NiPS_3}$. (c) The first derivative of spectral weight ω_p^2 obtained for the energy range of peak A (1.52–2.62 eV) and peaks B/C (2.63–5.00 eV). The Néel temperature of $\mathrm{NiPS_3}$ ($T_N \sim 154$ K) is represented as a red vertical line.

The optical conductivity of $\mathrm{NiPS_3}$ displays strong temperature (T) variations. Note that peak A shows strong enhancement in intensity, while peaks B and C sharpen without much change in intensity upon cooling. To quantify the temperature evolution, we calculated the squares of the plasma frequency ω_p^2: $\omega_p^2(T) = 8\int \sigma_1(\omega, T)d\omega$ [52], which we refer to as the spectral weight (SW). The optical sum rule is satisfied when we integrate up to 4.2 eV, implying the clear SW shifts from peak A to peaks B and C. At the same time, satisfaction of the optical sum rule indicates that most of the T-dependent changes in the electronic structure should occur near the Fermi level.

When we further examined the T dependence, we found clear anomaly in the SW changes of the main peaks occurring at T_N. Figure 1(c) shows the temperature derivative of SW in the energy ranges of peak A (1.52–2.63 eV) and of peaks B and C (2.63–5.00 eV). The former shows an abrupt change at T_N, and the latter shows a similar feature with the opposite trend, in which the shape is similar to the first derivative of $\chi(T)$ shown in Fig. 1(b). The observation of the SW anomaly at T_N is compelling evidence of strong coupling between the electronic and spin structures in $\mathrm{NiPS_3}$.

Conventionally, most ground states of strongly correlated compounds can be categorized via the Zaanen-Sawatzky-Allen (ZSA) classification scheme [53,54]. Depending on the relative size of on-site U and charge-transfer energy (Δ), the insulating ground state can be classified as either Mott-Hubbard or charge-transfer insulators. However, there is a less explored region in the ZSA scheme where compounds can have NCT energy ($\Delta < 0$). In this region, electrons of the ligand p orbital transfer to the TM d levels in the ground state, creating holes at the ligands without external doping. Thus, these compounds are often referred to as "self-doped" [55]. The ligand hole can contribute significantly to the conductivity and magnetism [30]. To some extent, the nature of the self-doped state is analogous to the ground state of the Zhang-Rice singlet states found in hole-doped cuprates [34,56,57].

Indeed, this interpretation of the self-doped ground state agrees with XAS and XPS results of $\mathrm{NiPS_3}$. We obtained the Ni $L_{2,3}$ edge XAS spectra of bulk $\mathrm{NiPS_3}$, which were subsequently analyzed using a cluster model. At the L_3 edge, $\mathrm{NiPS_3}$ shows a main peak near 851 eV [Fig. 2(a)]. It is clearly distinguished from those of compounds with large positive Δ values, such as NiO ($\Delta \sim 4.6$ eV), where the main peak shows clear splitting [58]. We simulated the Ni $L_{2,3}$ edge XAS spectra using a cluster model and found that $\mathrm{NiPS_3}$ belongs to the regime of $\Delta \leq 0$ eV [see Supplemental Material (e) [34]]. The XAS bulk spectral features remain at six layers, implying the overall ground state of the bulk persists down to at least a few layers. Additionally, the Ni $2p_{3/2}$ core XPS spectrum is nearly identical to that of $\mathrm{NiGa_2S_4}$, one of the first reported NCT sulfides [59–61] [Fig. 2(b)]. The $\mathrm{NiS_6}$ cluster model used on $\mathrm{NiGa_2S_4}$ also reproduces the Ni $2p_{3/2}$ XPS spectrum of $\mathrm{NiPS_3}$ well, using the parameters of $\Delta = -1.0$ eV and Coulomb interaction $U = 5.0$ eV. Note that the calculated ground state is given as $\Psi_g = \alpha|d^8\rangle + \beta|d^9\underline{L}\rangle + \gamma|d^{10}\underline{L}^2\rangle$, where $\underline{L}$ indicates a ligand (sulfur) hole, with $\alpha^2 = 0.25$, $\beta^2 = 0.60$, and $\gamma^2 = 0.15$. The above findings indicate that $\mathrm{NiPS_3}$ should have a self-doped ground state with dominant $d^9\underline{L}$ character, and demonstrate that $\mathrm{NiPS_3}$ is the only known example of a magnetically ordered vdW material with an NCT insulating state.

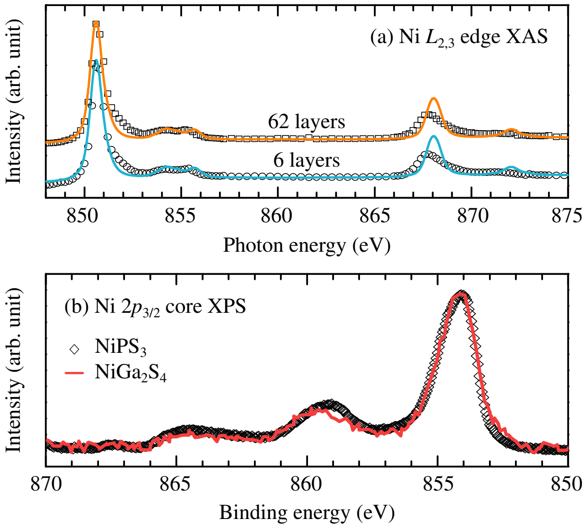

FIG. 2. (a) X-ray absorption spectra of 62- and 6-layer $\mathrm{NiPS_3}$ at the Ni $L_{2,3}$ edge. The L_3 edge is found near 851 eV, and the L_2 edge near 868 eV. The experimental data are represented in symbols, and the spectra calculated with the configuration-interaction cluster model using $U = 5$ eV, $\Delta = -1.0$ eV, and parameters following Ref. [59] are represented in solid lines. (b) The Ni $2p_{3/2}$ core x-ray photoemission spectra of $\mathrm{NiPS_3}$ from this Letter (symbols) and $\mathrm{NiGa_2S_4}$ from Ref. [59] (solid line). To facilitate this comparison, both spectra were normalized with respect to the main peak at 854 eV, and the Shirley background was removed in each case [34].

To gain further insights, we performed DFT + U_{eff} calculations. We used a magnetic ground state with zigzag AF ordering and a U_{eff} value of 4 eV [62]. The solid line in Fig. 3(a) shows the theoretical calculation of in-plane $\sigma_1(\omega)$ after rescaling the data to match the energy position of the first transition peak, while satisfying the sum rule. The theoretical $\sigma_1(\omega)$ reproduced most of the key features in our experimental data.

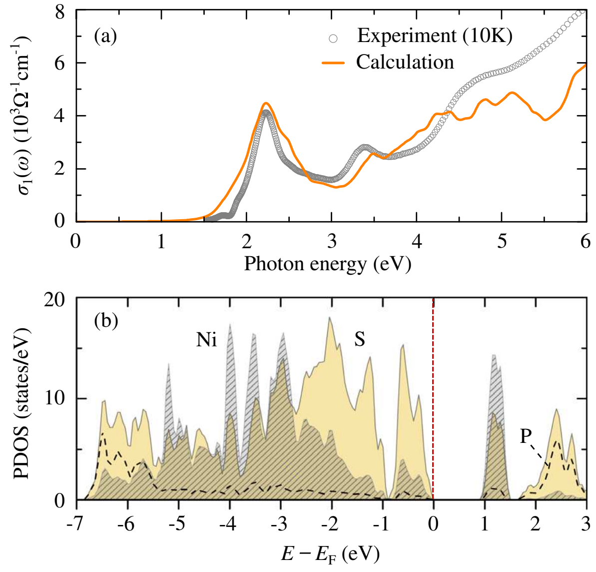

FIG. 3. (a) Real part of the optical conductivity $\sigma_1(\omega)$ obtained from experiments conducted at 10 K (circles) and from DFT+U_{eff} (solid line) after a stretch in the energy axis by 1.39 and a proper renormalization satisfying the sum rules [46]. (b) Projected density of states (PDOS) for Ni (gray oblique lines), S (yellow), and P (dashed line) obtained from DFT + U_{eff} calculations.

DFT $+ U_{\mathrm{eff}}$ calculations also support our interpretation of the self-doped NCT ground state in NiPS_3. Figure 3(b) shows the projected density of states (PDOS) for Ni, P, and S orbitals in NiPS_3. As shown by the dashed curve, the P $3p$ states are located mostly above 2 eV or below -5 eV and show a strong hybridization with the S $3p$ orbitals as a result of covalent bonding in the $(\mathrm{P}_2\mathrm{S}_6)^{4-}$ anion [48,49]. In contrast, the PDOSs for Ni and S orbitals are much higher near E_F than that of P $3p$ [Fig. 3(b)]. Thus, the valence bands near E_F are mainly S $3p$ orbital states, and the occupied Ni $3d$ orbital states are located mostly at lower energies. Narrow Ni $3d$ bands hybridized with the S $3p$ appear at $\sim$1.3 eV above E_{F}. The S $3p$ orbitals are located at higher energies than most Ni $3d$ orbitals, which may imply charge transfer from S to Ni *in the ground state* as a consequence of the NCT ground state [30].

The total number of d electrons from the PDOS analysis of our DFT $+ U_{\mathrm{eff}}$ was larger than expected from the formal valence. The Ni^{2+} ion from the formal valence predicts an occupation number of 8, while we obtained 8.6 from our PDOS analysis. This is consistent with a self-doped NCT ground state, where strong contributions from $d^9\underline{L}$ and $d^{10}\underline{L}^2$ configurations are expected in addition to d^8. Such an increase in the occupation number was also found in a DFT study of $\mathrm{Cs}_2\mathrm{Au}_2\mathrm{Cl}_6$, which showed a larger occupation number of d electrons than expected from the formal valence because $\Delta < 0$ [63].

The picture of the self-doped ground state also finds support from the magnetic properties. The value of the ordered magnetic moment from DFT $+ U_{\mathrm{eff}}$ is 1.24 μ_B per Ni ion, as opposed to the formal value of 2 μ_B. Such reduction in the moment is natural in view of the self-doped ground state that consists of three configurations, each with different spin numbers: d^8 ($S_{\mathrm{Ni}} = 1$), $d^9\underline{L}$ ($S_{\mathrm{Ni}} = 1/2$), and $d^{10}\underline{L}^2$ ($S_{\mathrm{Ni}} = 0$). The reduction in the moment may as well be a key to interpret the recent neutron diffraction experiment on NiPS_3 that reported the Ni moment in the ordered state of 1.05 μ_B [16]. While disorder and dimensional fluctuation in the quasi-2D system may reduce the ordered Ni moments by a certain amount, the self-doped ground state provides a consistent explanation on the reduced moment of Ni ions.

In previous $\chi(T)$ measurements, the effective magnetic moment of NiPS_3 in the paramagnetic state is known as 2.83 μ_B [64]. If we consider the spin of Ni ions only, this value is larger than the NCT picture anticipates. The effective moment, however, can vary substantially by how the T-independent susceptibility is analyzed [64–66]. According to our analysis, it varied at least from 2.49 μ_B to 2.89 μ_B [see Supplemental Material (b) [34]]. Our DFT $+ U_{\mathrm{eff}}$ calculations show finite spin polarizations not only at Ni but also at S sites. We think the spin moments localized at S sites can contribute to $\chi(T)$. A simple estimation from spin counting produces a moment of 2.34 μ_B [see Supplemental Material (a-4) [34]]. The enhancement in the effective moment may be another signature for the NCT ground state.

We can consider the T-dependent SW anomaly, shown in Fig. 1(c), within the simple cluster picture. In the $d^9\underline{L}$ state, the lowest energy transition, peak A, is expected to be enhanced when the neighboring Ni ions are bonded antiferromagnetically. The corresponding ground state should be composed of ${t_{2g}}^6{e_g}^3$ electrons at Ni $3d$ orbitals and one hole at S $3p$ orbitals ($\underline{L}$), i.e., ${t_{2g}}^6{e_g}^3$ with ${}^3A_{2g}$ symmetry [59]. According to the NiS_6 cluster model, the lowest-energy ionization state was found to have ${}^2E_g$ symmetry [59,67], and the corresponding state is clearly seen in the XPS valence spectra [see Supplemental Materials (e-3) [34]]. This suggests that peak A could be assigned as an intersite transition between NiS_6 clusters that transfer an electron between two ${t_{2g}}^6{e_g}^3\underline{L}$ (${}^3A_{2g}$) clusters. These transitions would split the ground state into a low-spin ${t_{2g}}^6{e_g}^2\underline{L}/{t_{2g}}^6{e_g}^3\underline{L}^2$ state on one site and a low-spin ${t_{2g}}^6{e_g}^3/{t_{2g}}^6{e_g}^4\underline{L}$ state on the other site. Considering spin conservation, such transitions may be allowed between AF-bonded clusters but forbidden between FM-bonded clusters [see Supplemental Material (f) [34]].

Therefore, the T-dependent *SW* and its anomaly should arise from the increased AF bonds in the zig-zag-ordered honeycomb lattice. At temperatures above T_N, there will be no preference between AF and FM bonds of NiS_6 clusters. Below T_N, however, the number of AF and FM bonds will differ: for the nearest neighboring Ni ions (with exchange interaction J_1), there will be two FM and one AF bond; for the second nearest (J_2), two FM and four AF bonds; and for the third nearest (J_3), three AF bonds only. Recent calculations on the monolayer of the NiPS_3 predicted that J_3 is nearly 4 times larger than J_1, while the value of J_2 is very small [12,68,69]. The dominant strength of J_3 is consistent with the increased number of AF bonds below T_N, and consequently the increased intensity of peak A. The SW, therefore, should reflect the degree of AF correlation present at a given temperature, which is consistent with the SW anomaly observed across T_N in the experiments [Fig. 1(c)]. In this regard, peak A of NiPS_3 can be used as an indicator for probing spin structure upon the increase of dimensional fluctuation in thin layers, or upon environmental change such as strain and electric or magnetic fields.

In conclusion, we investigated the electronic structure of NiPS_3, one of the layered vdW antiferromagnets. Our results revealed strong charge-spin coupling, i.e., a close relationship between the electronic structure and the magnetic ordering. We also found that NiPS_3 is a rare self-doped NCT insulator that exhibits a strong hole character in the ground state. The analysis of the optical conductivity based on the NCT state further demonstrated that the intercluster transition reflects the antiferromagnetic correlations among the neighboring Ni ions. Our findings demonstrate that strongly correlated electron physics can be explored using the material class of vdW magnets. Close inspection of the electronic structure of the vdW magnets is crucial to understanding the magnetic nature, which could lead to emergent phenomena and novel applications in spintronic devices.

We gratefully acknowledge insightful discussions with K. W. Kim, K. Burch, and B. C. Park. This work was supported by Institute for Basic Science (IBS) in Korea (Grants No. IBS-R009-D1 and No. IBS-R009-G1). S. Y. K. was supported by the Global Ph.D. Fellowship Program through the National Research Foundation of Korea (NRF) funded by the Ministry of Education (Grant No. NRF-2015H1A2A1034943). S. J. M. was supported by Basic Science Research Program through the NRF funded by the Ministry of Science, ICT and Future Planning (Grant No. 2017R1A2B4009413). T. Y. K. and C.-H. P. were supported by Korean Grant No. NRF-2016R1A1A1A05919979. KISTI Supercomputing Center (KSC-2017-S1-0011) provided computational resources. Experiments at PLS-II were supported in part by MSIP and POSTECH. The STXM experiment was supported by the National Council of Science and Technology (Grant No. CAP-16-01-KIST), and Grants No. NRF-2016K1A3A7A09005335 and No. NRF-2015R1A2A2A01007651. W. K. especially thanks N. Kim and H. Shin for their support for STXM measurement at PLS-II.

---

[*]jgpark10@snu.ac.kr
[†]soonjmoon@hanyang.ac.kr
[‡]twnoh@snu.ac.kr
[§]Measurement Science and Standards, National Research Council Canada, Ottawa, Ottawa K1A 0R6 Canada

[1] K. S. Novoselov, D. Jiang, F. Schedin, T. J. Booth, V. V. Khotkevich, S. V. Morozov, and A. K. Geim, Proc. Natl. Acad. Sci. U.S.A. **102**, 10451 (2005).
[2] K. S. Novoselov, A. K. Geim, S. V. Morozov, D. Jiang, Y. Zhang, S. V. Dubonos, I. V. Grigorieva, and A. A. Firsov, Science **306**, 666 (2004).
[3] A. K. Geim and I. V. Grigorieva, Nature (London) **499**, 419 (2013).
[4] X. Xi, L. Zhao, Z. Wang, H. Berger, L. Forró, J. Shan, and K. F. Mak, Nat. Nanotechnol. **10**, 765 (2015).
[5] K. F. Mak, K. He, J. Shan, and T. F. Heinz, Nat. Nanotechnol. **7**, 494 (2012).
[6] K. S. Novoselov, A. Mishchenko, A. Carvalho, and A. H. Castro Neto, Science **353**, aac9439 (2016).
[7] M. V. Sadavskii, Phys. Usp. **59**, 947 (2016).
[8] A. H. Castro Neto, Phys. Rev. Lett. **86**, 4382 (2001).
[9] X. Li and J. Yang, Natl. Sci. Rev. **3**, 365 (2016).
[10] C. Gong, L. Li, Z. Li, H. Ji, A. Stern, Y. Xia, T. Cao, C. Wang, Y. Wang, Z. Q. Qiu, R. J. Cava, S. G. Louie, and J. Xia, Nature (London) **546**, 265 (2017).
[11] N. Sivadas, M. W. Daniels, R. H. Swendsen, S. Okamoto, and D. Xiao, Phys. Rev. B **91**, 235425 (2015).
[12] B. L. Chittari, Y. Park, D. Lee, M. Han, A. H. Macdonald, E. Hwang, and J. Jung, Phys. Rev. B **94**, 184428 (2016).
[13] A. R. Wildes, K. C. Rule, R. I. Bewley, M. Enderle, and T. J. Hicks, J. Phys. Condens. Matter **24**, 416004 (2012).
[14] J.-U. Lee, S. Lee, J. H. Ryoo, S. Kang, T. Y. Kim, P. Kim, C.-H. Park, J. Park, and H. Cheong, Nano Lett. **16**, 7433 (2016).
[15] A. R. Wildes, B. Roessli, B. Lebech, and K. W. Godfrey, J. Phys. Condens. Matter **10**, 6417 (1998).
[16] A. R. Wildes, V. Simonet, E. Ressouche, G. J. McIntyre, M. Avdeev, E. Suard, S. A. J. Kimber, D. Lançon, G. Pepe, B. Moubaraki, and T. J. Hicks, Phys. Rev. B **92**, 224408 (2015).
[17] J. Park, J. Phys. Condens. Matter **28**, 301001 (2016).
[18] Additionally, the ferromagnetism in the monolayer has been reported in CrI_3; see B. Huang, G. Clark, E. Navarro-Moratalla, D. R. Klein, R. Cheng, K. L. Seyler, D. Zhong, E. Schmidgall, M. A. McGuire, D. H. Cobden, W. Yao, D. Xiao, P. Jarillo-Herrero, and X. Xu, Nature (London) **546**, 270 (2017).
[19] D. I. Khomskii, *Basic Aspects of the Quantum Theory of Solids* (Cambridge University Press, New York, 2010).
[20] D. I. Khomskii, *Transition Metal Compounds*, 1st ed. (Cambridge University Press, New York, 2014).
[21] D. N. Basov, R. D. Averitt, D. Van Der Marel, M. Dressel, and K. Haule, Rev. Mod. Phys. **83**, 471 (2011).
[22] J. G. Bednorz and K. A. Muller, Z. Phys. B **64**, 189 (1986).
[23] B. Keimer, S. A. Kivelson, M. R. Norman, S. Uchida, and J. Zaanen, Nature (London) **518**, 179 (2015).
[24] D. Neilson, A. Perali, and M. Zarenia, J. Phys. Conf. Ser. **702**, 012008 (2016).
[25] J. Sabio, J. Nilsson, and A. H. Castro Neto, Phys. Rev. B **78**, 075410 (2008).
[26] J. Crossno, J. K. Shi, K. Wang, X. Liu, A. Harzheim, A. Lucas, S. Sachdev, P. Kim, T. Taniguchi, K. Watanebe, T. A. Ohki, and K. C. Fong, Science **351**, 1058 (2016).
[27] J. H. Ngai, F. J. Walker, and C. H. Ahn, Annu. Rev. Mater. Res. **44**, 1 (2014).
[28] P. Zubko, S. Gariglio, M. Gabay, P. Ghosez, and J.-M. Triscone, Annu. Rev. Condens. Matter Phys. **2**, 141 (2011).
[29] A. J. Millis, in *Strong Interactions in Low Dimensions*, edited by D. Baeriswyl and L. Degiorgi (Kluwer Academic Publishers, Dordrecht, 2004), pp. 195–236.
[30] E. Pavarini, E. Koch, J. van den Brink, and G. Sawatzky, *Quantum Materials: Experiments and Theory* (Forschungszentrum Jülich, Germany, 2016), Vol. 6, ISBN 978-3-95806-159-0.
[31] D. Khomskii, Lith. J. Phys. **37**, 65 (1997).
[32] C. T. Kuo, M. Neumann, K. Balamurugan, H. J. Park, S. Kang, H. W. Shiu, J. H. Kang, B. H. Hong, M. Han, T. W. Noh, and J. G. Park, Sci. Rep. **6**, 20904 (2016).
[33] We subsequently checked the stoichiometry using a scanning electron microscope (COXI EM30; COXEM), equipped with an energy-dispersive x-ray spectrometer (Bruker Quantax 100), which was followed by magnetic susceptibility measurements obtained with a SQUID-VSM (MPMS 3; Quantum Design).
[34] See Supplemental Material at http://link.aps.org/supplemental/10.1103/PhysRevLett.120.136402, for experimental spectra and calculated results, which includes Refs. [35–40].
[35] K. Momma and F. Izumi, J. Appl. Crystallogr. **44**, 1272 (2011).

[36] C. Kittel, *Introduction to Solid State Physics* 8th ed. (John Wiley and Sons, New York, 2004).

[37] S. Blundell, *Magnetism in Condensed Matter* (Oxford University Press, New York, 2001).

[38] T. Mizokawa, A. Fujimori, H. Namatame, K. Akeyama, and N. Kosugi, Phys. Rev. B **49**, 7193 (1994).

[39] V. Bisogni, S. Catalano, R. J. Green, M. Gibert, R. Scherwitzl, Y. Huang, V. N. Strocov, P. Zubko, S. Balandeh, J. Triscone, G. Sawatzky, and T. Schmitt, Nat. Commun. **7**, 13017 (2016).

[40] E. Stavitski and F. M. F. De Groot, Micron **41**, 687 (2010).

[41] S. L. Dudarev, G. A. Botton, S. Y. Savrasov, C. J. Humphreys, and A. P. Sutton, Phys. Rev. B **57**, 1505 (1998).

[42] D. R. Hamann, Phys. Rev. B **88**, 085117 (2013).

[43] M. Schlipf and F. Gygi, Comput. Phys. Commun. **196**, 36 (2015).

[44] J. P. Perdew, K. Burke, and M. Ernzerhof, Phys. Rev. Lett. **77**, 3865 (1996).

[45] A. Marini, C. Hogan, M. Gruning, and D. Varsano, Comput. Phys. Commun. **180**, 1392 (2009).

[46] Z. H. Levine and D. C. Allan, Phys. Rev. Lett. **63**, 1719 (1989); R. Del Sole and R. Girlanda, Phys. Rev. B **48**, 11789 (1993).

[47] P. Giannozzi, S. Baroni, N. Bonini, M. Calandra, R. Car, C. Cavazzoni, D. Ceresoli, G. L. Chiarotti, M. Cococcioni, I. Dabo, A. D. Corso, S. Fabris, G. Fratesi, S. de Gironcoli, R. Gebauer, U. Gerstmann, C. Gougoussis, A. Kokalj, M. Lazzeri, L. Martin-Samos, N. Marzari, F. Mauri, R. Mazzarello, S. Paolini, A. Pasquarello, L. Paulatto, C. Sbraccia, S. Scandolo, G. Sclauzero, A. P. Seitsonen, A. Smogunov, P. Umari, and R. M. Wentzcovitch, J. Phys. Condens. Matter **21**, 395502 (2009).

[48] R. Brec, Solid State Ionics **22**, 3 (1986).

[49] M. Piacentini, V. Grasso, S. Santangelo, M. Fanfoni, S. Modesti, and A. Savoia, Solid State Commun. **51**, 467 (1984).

[50] Fabry-Pérot interference fringes are observed in a narrow energy range near 1.4 eV and below 0.9 eV, where the sample becomes transparent; these are not shown.

[51] R. Newman and R. Chrenko, Phys. Rev. **114**, 1507 (1959).

[52] M. Dressel and G. Gruner, *Electrodynamics of Solids: Optical Properties of Electrons in Matter* (Cambridge University Press, New York, 2002).

[53] J. Zaanen, G. A. Sawatzky, and J. W. Allen, Phys. Rev. Lett. **55**, 418 (1985).

[54] A. E. Bocquet, T. Mizokawa, T. Saitoh, H. Namatame, and A. Fujimori, Phys. Rev. B **46**, 3771 (1992).

[55] M. A. Korotin, V. I. Anisimov, D. I. Khomskii, and G. A. Sawatzky, Phys. Rev. Lett. **80**, 4305 (1998).

[56] C. Monney, V. Bisogni, K. J. Zhou, R. Kraus, V. N. Strocov, G. Behr, S. L. Drechsler, H. Rosner, S. Johnston, J. Geck, and T. Schmitt, Phys. Rev. B **94**, 165118 (2016).

[57] D. Choudhury, P. Rivero, D. Meyers, X. Liu, Y. Cao, S. Middey, M. J. Whitaker, S. Barraza-Lopez, J. W. Freeland, M. Greenblatt, and J. Chakhalian, Phys. Rev. B **92**, 201108 (2015).

[58] G. van der Laan, J. Zaanen, G. A. Sawatzky, R. Karnatak, and J.-M. Esteva, Phys. Rev. B **33**, 4253 (1986).

[59] K. Takubo, T. Mizokawa, J. Y. Son, T. Nambu, S. Nakatsuji, and Y. Maeno, Phys. Rev. Lett. **99**, 037203 (2007).

[60] S. Nakatsuji, Y. Nambu, H. Tonomura, O. Sakai, S. Jonas, C. Broholm, H. Tsunetsugu, Y. Qiu, and Y. Maeno, Science **309**, 1697 (2005).

[61] It seems that the lower electronegativity of chalcogen ions in TMTC can also drive the system into the NCT regime, as in the cases of some TM oxides [30,55–57].

[62] A direct comparison between U values in the configuration interaction cluster model and U_{eff} values in DFT $+ U_{\mathrm{eff}}$ calculations is difficult due to fundamental differences between the two methods; however, the parameters for each model are within the typical values used for Ni compounds.

[63] A. V Ushakov, S. V Streltsov, and D. I. Khomskii, J. Phys. Condens. Matter **23**, 445601 (2011).

[64] P. A. Joy and S. Vasudevan, Phys. Rev. B **46**, 5425 (1992).

[65] G. Le Flem, R. Brec, G. Ouvard, A. Louisy, and P. Segransan, J. Phys. Chem. Solids **43**, 455 (1982).

[66] B. E. Taylor, J. Steger, and A. Wold, J. Solid State Chem. **7**, 461 (1973).

[67] K. Takubo, T. Mizokawa, Y. Nambu, and S. Nakatsuji, Phys. Rev. B **79**, 134422 (2009).

[68] The calculated exchange interaction strength of bulk $NiPS_3$ in our work also gave results for J_1, J_2, and J_3 that are similar to those for the monolayer [11,12].

[69] Research on $NiGa_2S_4$ revealed that the hole character in the S $3p$ can raise the J_3 [59]. Similarly, the enhancement of J_3 may be another consequence of the NCT nature of $NiPS_3$.